Inorganic Chemistry

Article

pubs.acs.org/IC

Tri(pyridylmethyl)phosphine: The Elusive Congener of TPA Shows Surprisingly Different Coordination Behavior

Christopher J. Whiteoak, James D. Nobbs, Evgeny Kiryushchenkov, Sandro Pagano, Andrew J.P. White, and George J.P. Britovsek*

Department of Chemistry, Imperial College London, Exhibition Road, London SW7 2AY, United Kingdom

Supporting Information

ABSTRACT: Tri(pyridylmethyl)phosphine (TPPh), the remarkably elusive congener of tri(pyridylmethyl)amine (TPA), has been prepared, as well as the relative tri(*N*-methylpyridylamino)phosphine (TPAMP). The coordination properties of these new ligands have been evaluated for chromium(III), iron(II), and ruthenium(II) complexes and compared with the related TPA complexes. In all cases, a different coordination behavior has been observed whereby TPPh and TPAMP always act as tridentate ligands. A chromium(III) complex $[Cr(TPPh)Cl_3]$ has been prepared, which has shown low ethylene oligomerization activity. Octahedral low spin iron(II) complexes $[Fe(TPPh)_2]^{2+}$ and $[Fe(TPAMP)_2]^{2+}$ were obtained with two ligands bound to the metal center. Ruthenium(II) chloro complexes of TPA and TPPh undergo ligand exchange reactions in acetonitrile, and the ruthenium(II) complex $[Ru(MeCN)_2(TPA)]^{2+}$ can be oxidized by *m*-CPBA in acetonitrile to give a transient ruthenium(IV) oxo complex $[Ru(O)(MeCN)(TPA)]^{2+}$. Attempts to generate high valent ruthenium(IV) oxo TPPh or TPAMP complexes could not be achieved, probably due to insufficient stabilization by these strong field ligands.

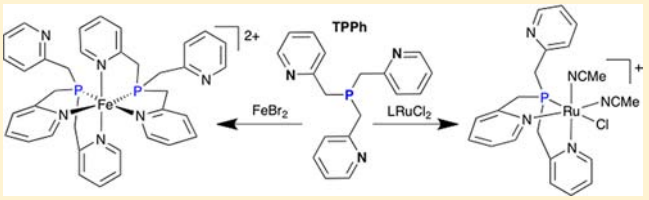

INTRODUCTION

Tetradentate tripodal ligands are an important ligand class in coordination chemistry, and tripodal tripyridyl ligands in particular have received widespread application in catalysis and materials chemistry.[1,2] Tri(pyridylmethyl)amine (TPA)[3] has acquired iconic status, and many transition metal complexes containing TPA are known today (Figure 1). In most

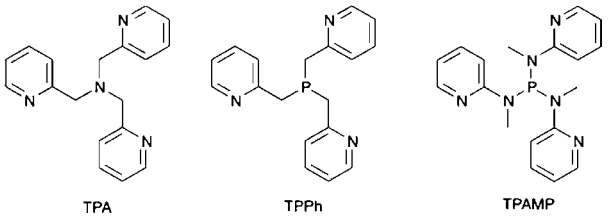

Figure 1. Tripodal ligands TPA, TPPh, and TPAMP.

complexes, TPA coordinates in a tetradentate fashion, although some examples are known where TPA acts as a tridentate ligand.[4−8] Metal complexes have been prepared with either one or with two TPA ligands.[5,9,10]

Iron TPA complexes, including many derivatives, have been investigated extensively as catalysts in alkane and alkene oxidation.[11−18] We have previously reported a systematic study on pyridine versus amine donors in TPA and related ligands and their effect on the catalytic oxidation properties of their respective iron(II) complexes.[19] Alkane and alkene oxidation catalysts with TPA ligands have also been used with other metals, notably ruthenium[20−26] and nickel.[27] An important feature of the TPA ligand appears to be the ability to stabilize high valent metal complexes such as Fe(IV), Ru(IV), and Re(V) oxo complexes, which are often invoked as intermediates in oxidation catalysis.[4,24,28] This has led to the development of catalytic systems based on ruthenium complexes with polypyridyl ligands including TPA that, in combination with a chemical oxidant, are able to oxidize hydrocarbons.[29−31] Particularly interesting are recent reports on the use of water as the oxygen source in hydrocarbon oxygenations or indeed the oxidation of water, using ruthenium TPA complexes in combination with the one-electron oxidant cerium ammonium nitrate (CAN),[23,32−34] or the photogenerated oxidant $[Ru(bipy)_3]^{3+}$.[35,36]

Many modifications to the TPA ligand have been reported, either to the pyridyl moieties,[1] or to the linkers between the pyridine and the central amine.[37] The higher congener, tri(pyridylmethyl)phosphine (TPPh),[38] where the central nitrogen donor is substituted for a phosphorus, has so far remained remarkably elusive (Figure 1). The only sighting of TPPh was reported by Chiswell in 1967.[39] TPPh was reportedly obtained by the reaction of 3 equiv of α-picolyl lithium with 1 equiv of PCl_3 in 5% yield, but aside from elemental analysis, no characterization was provided. Manganese(II), nickel(II), and cobalt(II) complexes were reported and analyzed as $[MCl(TPPh)]X$ (X = Cl^- or ClO_4^-) according to elemental analysis. As will be shown here, these results are highly questionable, and to the best of

Received: February 27, 2013
Published: May 23, 2013

   dx.doi.org/10.1021/ic4005196 | *Inorg. Chem.* 2013, 52, 7000−7009

our knowledge, there are no other reports in the literature on the synthesis of TPPh or its metal complexes. This is surprising, considering the popularity of TPA and that related mono- and bis(pyridylmethyl)phosphine ligands and their metal complexes have been known for some time,[40−49] as well as the ethylene-bridged tri(pyridylethyl)phosphine.[50]

We present here the first reliable and high yielding synthesis for TPPh. In order to increase the basicity of the central donor, we also prepared the tri(pyridylamine)phosphine ligand TPAMP (see Figure 1). This ligand also appears to be new, although the unmethylated ligand[51] as well as several mono- and bis(pyridylamine)phosphine derivatives have been reported.[40,44,52−54]

The coordination behavior of the TPPh and TPAMP ligands has been investigated for several transition metals including chromium, iron, and ruthenium and compared with their TPA analogues. In the case of ruthenium(II) TPPh and TPAMP complexes, the formation of high-valent ruthenium(IV) oxo complexes has been investigated using both electrochemical and chemical methods, and the results have been compared with ruthenium(II) TPA complexes. Both TPPh and TPAMP show a surprisingly different coordination behavior compared with TPA.

RESULTS AND DISCUSSION

Synthesis of Ligands. Several attempts to repeat the synthesis of TPPh as described by Chiswell in 1967 failed in our hands, which was not surprising considering the reported yield of 0−5%.[39] In our first alternative approach, $P(SiMe_3)_3$ was reacted with 3 equiv of freshly prepared 2-picolylchloride in dichloromethane. The product that was isolated was the novel salt tetra(pyridylmethyl)phosphonium chloride in 33% yield (eq 1.). Similar observations have been made in related

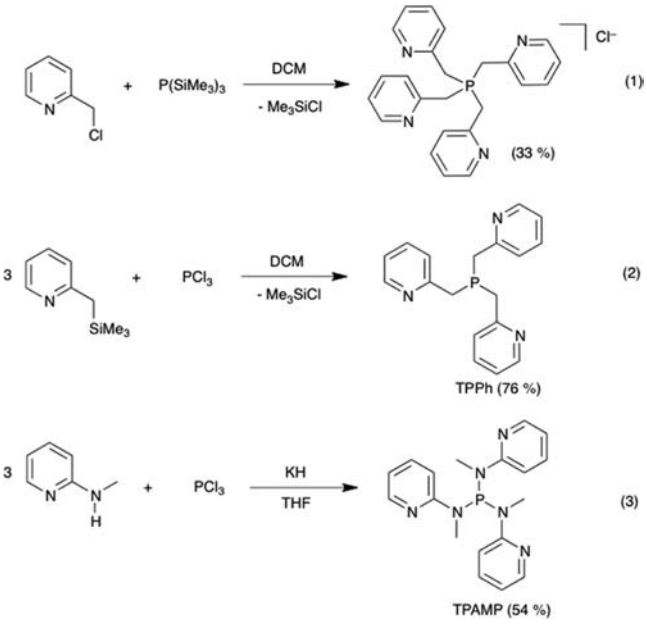

reactions with $P(SiMe_3)_3$.[55−57] The ^{1}H NMR spectrum contains a doublet at 4.71 ppm for the methylene protons ($^2J_{HP}$ = 16.0 Hz), in addition to the aromatic signals, and the ^{31}P NMR spectrum has one resonance at δ 32.6 ppm (see Supporting Information).

The synthesis of TPPh was achieved by the reaction of 3 equiv of 2-(trimethylsilylmethyl)pyridine[58] with 1 equiv of PCl_3 (eq 2). After workup, TPPh was obtained in high purity and 76% yield, and the ^{1}H NMR spectrum contains four resonances for the pyridyl group and a doublet for the methylene bridge at 3.12 ppm with $^2J_{HP}$ = 1.2 Hz, a much smaller coupling than that for the phosphonium salt. The ^{31}P NMR spectrum shows one resonance at −13.0 ppm. The melting point is 81 °C, which is significantly lower than the value of 115−120 °C reported by Chiswell,[39] and we therefore do not believe that TPPh was cleanly obtained by his method.

Tri(*N*-methyl-pyridylamino)phosphine (TPAMP) was prepared by the reaction of the potassium salt of *N*-methylamino pyridine with PCl_3 in THF and obtained as a white powder in 54% yield (eq 3). The methyl signal is observed at 3.00 ppm with a small coupling of $^3J_{HP}$ = 2 Hz, and the ^{31}P NMR spectrum shows a singlet at 96.8 ppm.

Synthesis of Chromium and Iron Complexes. In order to explore the coordination properties of the new ligands TPPh and TPAMP, several transition metal complexes have been prepared. For TPA, mononuclear Cr(II) and Cr(III) complexes have been reported previously, including X-ray analyses of $[CrCl_2(TPA)]$ and $[CrCl_2(TPA)](BPh_4)$, where TPA acts as a tetradentate ligand.[59] Here, the reaction of TPPh with $CrCl_3$·3THF in THF resulted in the formation of the complex $[CrCl_3(TPPh)]$ (eq 4). The complex was analyzed by IR, MS,

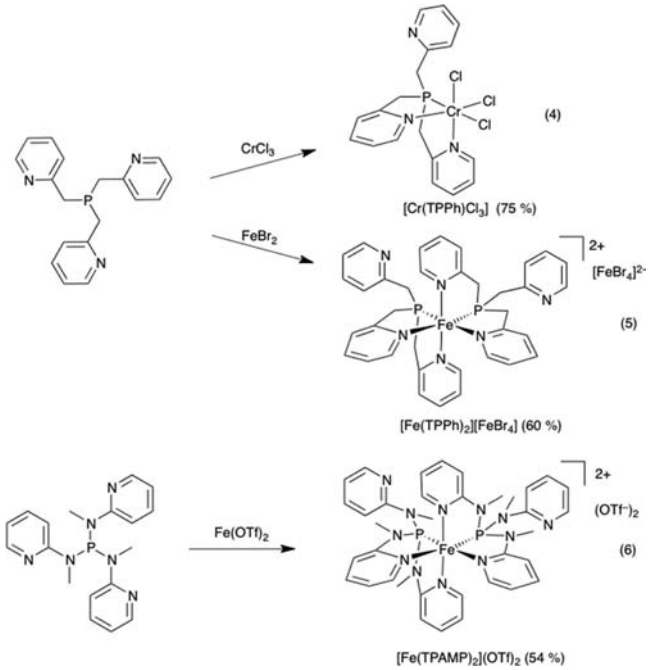

CHN analysis and single crystal X-ray diffraction, which revealed a tridentate coordination mode as shown in Figure 2. One of the pyridyl arms does not coordinate to the metal center, and the ligand adopts a facial coordination mode. The coordination is very similar to that observed in the related chromium complex with the tridentate bis(pyridylmethyl)-phenylphosphine ligand.[45,46] Noticeably, the Cr−P−CH_2 angle for the noncoordinated arm is substantially larger at 122.25(5)° than those to the coordinated arms [102.97(5)° and 103.72(5)°]. A similar pattern, but to a lesser extent, is seen in the structure of the chromium(II) complex $[CrCl_2(TPA)]$, where the Cr−N−CH_2 angle for the loosely bound pyridyl arm [112.6° and 113.7° for the two independent complexes] is larger than those of the coordinated arms [105.3° to 107.1°].[59]

dx.doi.org/10.1021/ic4005196 | Inorg. Chem. 2013, 52, 7000−7009

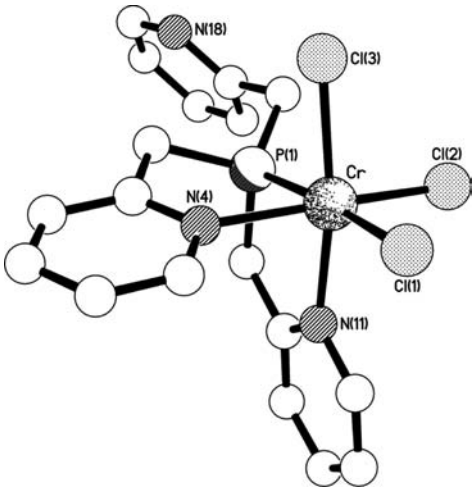

Figure 2. Crystal structure of $[CrCl_3(TPPh)]$. Selected bond lengths (Å) and angles (deg): Cr−Cl(1) 2.3481(4), Cr−Cl(2) 2.3119(4), Cr−Cl(3) 2.3004(4), Cr−P(1) 2.3333(4), Cr−N(4) 2.1486(11), Cr−N(11) 2.1256(11), P(1)−Cr−N(4) 78.62(3), P(1)−Cr−N(11) 81.42(3), N(4)−Cr−N(11) 85.17(4).

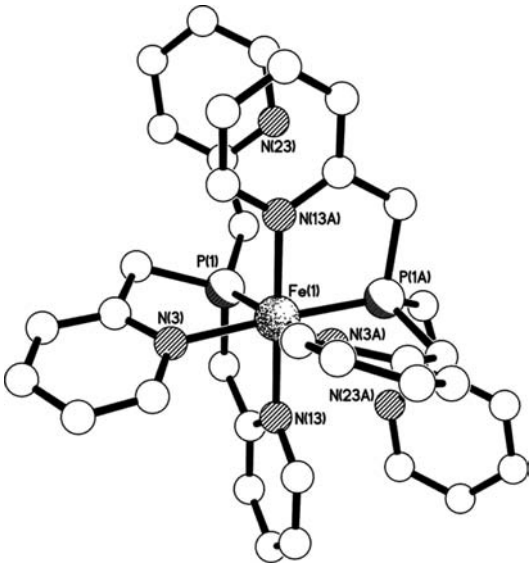

Figure 3. Structure of the C_2-symmetric cation present in the crystals of $[Fe(TPPh)_2][FeBr_4]$. Selected bond lengths (Å) and angles (deg): Fe(1)−P(1) 2.1547(11), Fe(1)−N(3) 2.085(3), Fe(1)−N(13) 2.021(3), P(1)−Fe(1)−N(3) 82.09(9), P(1)−Fe(1)−N(13) 85.95(10), N(3)−Fe(1)−N(13) 83.88(12).

The Cr−P bond in the TPPh complex [2.3333(4) Å] is longer than the corresponding Cr−N bond in the TPA complex [2.152(5) and 2.164(5) Å]. The chromium(III) complex $[CrCl_2(TPA)](BPh_4)$ has all three pyridyl arms coordinated to the metal center, with associated Cr−N−CH_2 angles of *ca.* 106.7°, 107.2°, and 109.7°. This pattern of two similar and one larger M−N−CH_2 angles is seen in many complexes with a tetradentate TPA ligand (see Table S1).

NMR analysis did not provide any meaningful characterization due to severe paramagnetic line broadening. Our interest in chromium-based ethylene oligomerization catalysts[60,61] prompted us to assess the activity of $[CrCl_3(TPPh)]$ for the oligomerization of ethylene, using 500 equiv MAO as the cocatalyst. A low activity of only 10 g/mmolhbar was observed, similar to the activities reported for chromium complexes of TPA and bis(pyridylmethyl)phenylphosphine.[49,59]

The reaction of TPPh with $FeBr_2$ in acetonitrile at room temperature results in a brick-red product (eq 5). The ^{1}H NMR spectrum shows resonances in the diamagnetic region, indicative of a low spin iron(II) complex. However, the signals are broad which suggests the presence of a paramagnetic species or fluxional behavior. The ^{31}P NMR spectrum displays a single resonance at 96.4 ppm, which is a significant change from −13.0 ppm for TPPh. Crystals suitable for single crystal X-ray crystallography were obtained by slow diffusion of diethylether into a concentrated solution of the complex in acetonitrile. The product was not a mono-ligand complex, but a combination of a bis-ligand dicationic iron(II) complex together with a dianionic iron(II) tetrabromide complex $[Fe(TPPh)_2][FeBr_4]$ (see Figure 3). The TPPh ligand coordinates again as a tridentate ligand, and the cationic complex has crystallographic C_2 symmetry. As was seen for $[CrCl_3(TPPh)]$, the M−P−CH_2 angle for the noncoordinated arm is substantially larger [133.12(17)°] than those to the coordinated arms [102.66(13)° and 103.84(14)°]. The six-coordinate $[Fe(TPPh)_2]^{2+}$ cation is related to the $[Fe(TPA)_2]^{2+}$ complex, previously reported by Hagen,[5] which shows a similar coordination, but less pronounced. The Fe−N−CH_2 angles for the noncoordinated pyridyl arms are *ca.* 111.6° and 115.3°, while those for the coordinated arms range between 103.7° and 107.9°. The bonds to the central atom of the ligand (P for TPPh, and N for TPA) are very different for $[Fe(TPPh)_2][FeBr_4]$ [2.1547(11) Å] compared to $[Fe(TPA)_2](OTf)_2$ [2.317(5) and 2.330(5) Å]. The different ligand field strength of P versus N donors results in a low spin complex in the case of $[Fe(TPPh)_2]^{2+}$ and a high spin complex for $[Fe(TPA)_2]^{2+}$. Metal ligand bond lengths are typically 10% shorter for low spin iron(II) complexes, compared to high spin analogues. Consequently, the Fe−N_{pyr} bonds are also noticeably shorter in the low spin cation $[Fe(TPPh)_2]^{2+}$ [2.021(3) and 2.085(3) Å] compared to the high spin cation $[Fe(TPA)_2]^{2+}$ [2.134(5)−2.215(5) Å].[5] In both cases, the central donors N versus P are *cis* to each other. The presence of the paramagnetic anion $[FeBr_4]^{2-}$ is likely to be the reason for the signal broadening in the ^{1}H NMR spectrum of $[Fe(TPPh)_2][FeBr_4]$.

The reaction of TPAMP with $Fe(OTf)_2$ in THF resulted in a similar bis-ligand complex $[Fe(TPAMP)_2](OTf)_2$. Despite the 1:1 ratio between iron and ligand used in the synthesis, the formation of the bis(ligand) complex appears to be thermodynamically preferred (eq 6). The ^{1}H NMR spectrum shows 12 aromatic signals and two N-methyl signals for two coordinated and one uncoordinated pyridine units. Single crystals were obtained from acetonitrile/diethyl ether. The low spin cations in the structures of $[Fe(TPAMP)_2](OTf)_2$ (Figure 4) and its analogue $[Fe(TPAMP)_2][FeCl_4]_2$ (see below and the Supporting Information) are similar to that observed for $[Fe(TPPh)_2][FeBr_4]$. Each TPAMP ligand binds in a tridentate fashion with one of the pyridyl arms not bound to the metal, with the Fe−P−N angle for this noncoordinated arm being in each case substantially larger [in the range 133.45(6)−136.36(6)° across all the independent TPAMP ligands in both structures] than those for the coordinated arms [which range between 102.17(11)° and 104.65(5)°]. The Fe−P bonds to the central phosphorus atom in each ligand [2.0972(9)−2.1154(4) Å] are shorter than that seen in the TPPh complex [2.1547(11) Å], although the Fe−N(py) bonds are compara-

dx.doi.org/10.1021/ic4005196 | *Inorg. Chem.* 2013, 52, 7000−7009

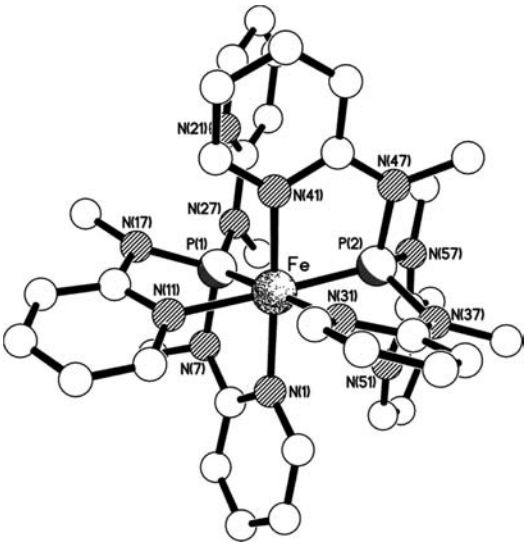

Figure 4. Structure of the cation present in the crystals of $[Fe(TPAMP)_2](OTf)_2$. Selected bond lengths (Å) and angles (deg): Fe–P(1) 2.1050(4), Fe–P(2) 2.1154(4), Fe–N(1) 2.0088(14), Fe–N(11) 2.0865(13), Fe–N(31) 2.0963(13), Fe–N(41) 2.0077(14), P(1)–Fe–N(1) 84.64(4), P(1)–Fe–N(11) 78.99(4), N(1)–Fe–N(11) 83.01(5), P(2)–Fe–N(31) 78.18(4), P(2)–Fe–N(41) 84.76(4), N(31)–Fe–N(41) 84.58(5).

ble, ranging between 1.990(3) and 2.0963(13) Å in the TPAMP complex, *cf.* 2.021(3) and 2.085(3) in $[Fe(TPP)_2][FeBr_4]$.

The reaction of TPAMP with $FeCl_3$ in DCM resulted in a red solid, which according to MS and elemental analysis corresponds to the complex $[FeCl_3(TPAMP)]$, probably similar to the chromium(III) complex mentioned above. Attempts to crystallize this complex resulted in single crystals, which upon analysis gave $[Fe(TPAMP)_2][FeCl_4]_2$ (see Supporting Information). This compound contains iron(II) in the cation and iron(III) in the anion. Reduction of one of the iron(III) centers to iron(II) presumably took place during the crystallization process, but the origin of this reduction is unclear at this stage.

Synthesis of Ruthenium(II) Complexes. The reaction of TPA and $[RuCl_2(p\text{-cymene})]_2$ in acetonitrile was expected to give either $[RuCl_2(TPA)]$, in analogy to the reaction of TPA with $FeCl_2$,[18] or $[RuCl(MeCN)(TPA)]Cl$, analogous to the reaction between $[RuCl_2(PhCN)_4]$ and TPA, which gave $[RuCl(PhCN)(TPA)]Cl$.[25] However, the ^1H NMR spectra in CD_3CN and in CD_2Cl_2 indicate the presence of multiple species (see Figure S1). A solution of the product in CD_3CN was monitored by ^1H NMR spectroscopy over time (17 days), and the region of the CH_2 protons is shown in Figure 5. Three species, **A**, **B**, and **C**, can be distinguished. Each species shows a double doublet (AB pattern) for the two pyridylmethyl arms *trans* to each other and a singlet for the other pyridylmethyl group, a common motif that is also observed in other ruthenium(II) TPA complexes.[7,25] Species **A**, which is least abundant and shows two doublets at 5.09 and 5.25 ppm (J_{AB} = 15.2 Hz) together with a singlet at 4.73 ppm, is assigned to $[RuCl_2(TPA)]$. Product **B** with two doublets at 4.77 and 5.37 ppm (J_{AB} = 14.6 Hz) and a singlet at δ 4.61 ppm is assigned to $[RuCl(MeCN)(TPA)]Cl$. Only one isomer of this complex is observed, most likely the isomer with MeCN *trans* to a pyridine due to the stronger *trans* labilizing effect of pyridine compared

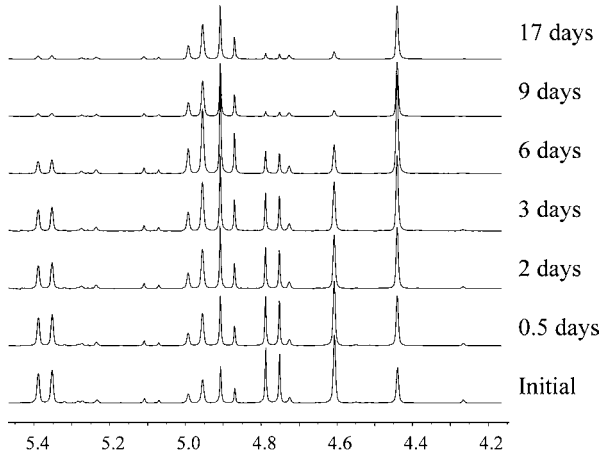

Figure 5. ^1H NMR spectra of the CH_2 region of the reaction of $[RuCl_2(TPA)]$ in CD_3CN over time at 298 K.

to an amine donor. A third species **C** with two AB doublets at δ 4.89 and 4.97 ppm (J_{AB} = 15.1 Hz) and a singlet at δ 4.44 ppm is assigned as $[Ru(MeCN)_2(TPA)]Cl_2$. During the first 24 h, the color changes from red to yellow, and the mixture gradually evolves into essentially **C** only.

A solution of the product in dichloromethane yielded red crystals, which were analyzed by X-ray crystallography as $[RuCl_2(TPA)]$ (**A**). The initial red product is therefore complex **A**, which slowly undergoes substitution of the chloride ligands for MeCN ligands, to give the yellow complexes **B** and **C**, as shown in eq 7. Despite several attempts, it was not

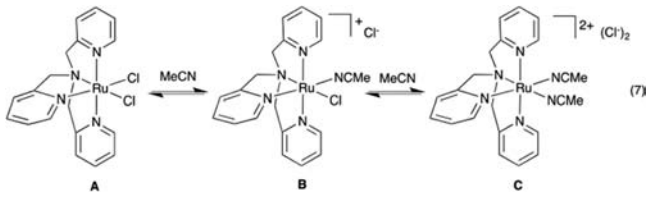

possible to isolate complex **B** or **C** in pure form. Noteworthy, only one isomer has been reported from the reaction of $[RuCl_2(PhCN)_4]$ with TPA in methanol, which was assigned as $[RuCl(PhCN)(TPA)]Cl$, analogous to isomer **B**.[25]

The molecular structure of the mononuclear dichloro ruthenium(II) complex $[RuCl_2(TPA)]$ (**A**) is shown in Figure 6, together with the relevant bond lengths and angles. The structure is similar to the Ru(III) analogue $[RuCl_2(TPA)](ClO_4)$ and the cationic Ru(II) complexes $[RuCl(S\text{-}DMSO)(TPA)](PF_6)$ and $[RuCl(TPA)]_2(ClO_4)_2$, although the Ru–N bonds in $[RuCl_2(TPA)]$ are slightly shorter.[20,26,62] The Ru–N–CH_2 angles for the tetradentate TPA ligand in these three mononuclear structures show the same pattern as seen for the first row metal TPA complexes, with two similar angles ranging between *ca.* 105.2° and 106.4(4)° and one larger angle of 110.0(4)°, 110.05(12)°, and *ca.* 111.4°. For the dimeric complex $[RuCl(TPA)]_2(ClO_4)_2$, the same pattern is present but to a lesser extent, with the three Ru–N–CH_2 angles being *ca.* 106.2°, 106.5°, and 107.8° (Table 1).

Despite the mixture of three species **A**, **B**, and **C**, exchange of the Cl^- anions for noncoordinating SbF_6^- counterions in acetonitrile results in a single complex $[Ru(MeCN)_2(TPA)](SbF_6)_2$, whose ^1H NMR spectrum is very similar to the spectrum of complex **C**, which was assigned as $[Ru(MeCN)_2(TPA)]Cl_2$ (See Figure S2). The *ortho* protons of

dx.doi.org/10.1021/ic4005196 | *Inorg. Chem.* 2013, 52, 7000–7009

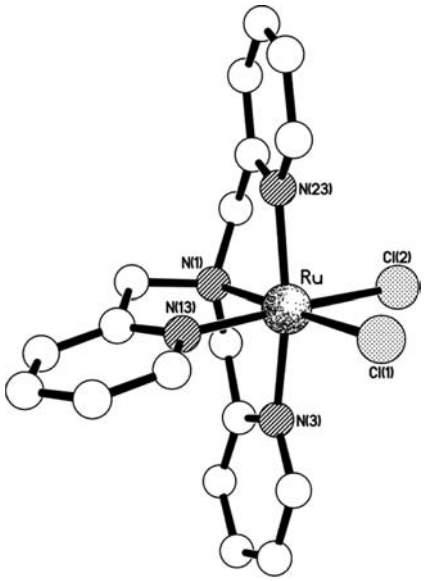

Figure 6. Crystal structure of $[RuCl_2(TPA)]$. Selected bond lengths (Å) and angles (deg): Ru−Cl(1) 2.4558(5), Ru−Cl(2) 2.4473(5), Ru−N(1) 2.0529(17), Ru−N(3) 2.0534(18), Ru−N(13) 2.0279(18), Ru−N(23) 2.0471(17), N(1)−Ru−N(3) 83.26(7), N(1)−Ru−N(13) 83.20(7), N(1)−Ru−N(23) 81.34(7), N(3)−Ru−N(13) 85.36(7), N(3)−Ru−N(23) 164.57(7), N(13)−Ru−N(23) 93.78(7).

all three pyridine moieties appear in a 2:1 ratio and are shifted downfield compared to the free ligand. Two signals are observed for coordinated acetonitrile ligands, which implies that TPA is coordinated as a tetradentate ligand. Single crystals were obtained of complex $[Ru(MeCN)_2(TPA)](SbF_6)_2$, and the molecular structure is shown in Figure 7. The structure of $[Ru(MeCN)_2(TPA)](SbF_6)_2$ is very similar to that of the

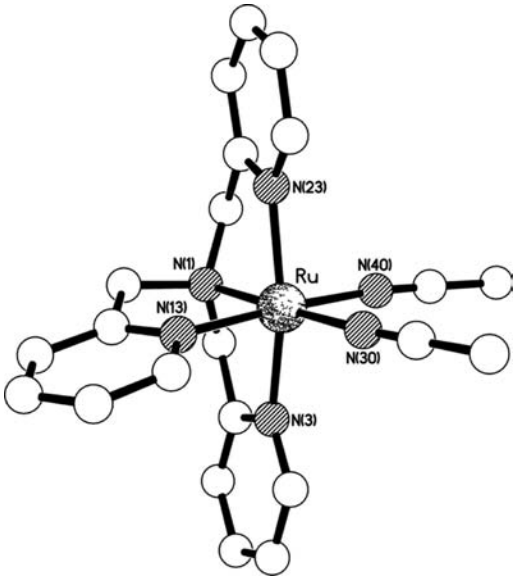

Figure 7. Structure of the cation present in the crystals of $[Ru(MeCN)_2(TPA)](SbF_6)_2$. Selected bond lengths (Å) and angles (deg): Ru−N(1) 2.0628(18), Ru−N(3) 2.0681(17), Ru−N(13) 2.0427(18), Ru−N(23) 2.0693(17), Ru−N(30) 2.0448(18), Ru−N(40) 2.0376(19), N(1)−Ru−N(3) 82.65(7), N(1)−Ru−N(13) 82.71(7), N(1)−Ru−N(23) 81.47(7), N(3)−Ru−N(13) 85.08(7), N(3)−Ru−N(23) 164.09(7), N(13)−Ru−N(23) 93.89(7).

neutral analogue $[RuCl_2(TPA)]$, with the TPA ligand coordinated in a tetradentate fashion with the same pattern for the Ru−N−CH_2 angles, though the Ru−N bonds in the cationic complex are slightly larger than in the neutral species.

The reaction of TPPh with $[RuCl_2(p\text{-cymene})]_2$ in acetonitrile results in the formation of $[RuCl(MeCN)_2(TPPh)]Cl$ (see Scheme 1). The ^1H NMR spectrum for $[RuCl(MeCN)_2(TPPh)]Cl$ at 283 K in CD_3CN shows two different environments for the pyridine protons in a 2:1 ratio, whereby the minor set of signals is broadened (see Figure S3). The CH_2 protons appear as two sets of signals in a ratio of 2:1, but surprisingly, in this case the major signals are broadened. There is no change to the spectrum when the temperature is decreased, but at higher temperatures, the broad signals sharpen. We propose that this fluxionality is due to a ligand exchange process between $[RuCl(MeCN)_2(TPPh)]Cl$ and the dicationic complex $[Ru(MeCN)_3(TPPh)]Cl_2$, as indicated in Scheme 1.

The reaction of TPAMP with $[RuCl_2(p\text{-cymene})]_2$ in acetonitrile gives a complex that shows no fluxional behavior as seen for $[RuCl(MeCN)_2(TPPh)]Cl$. The ^1H NMR spectrum is very similar to that of $[Ru(MeCN)_3(TPAMP)](SbF_6)_2$ (see below), which suggests that this complex exists mainly as $[Ru(MeCN)_3(TPAMP)](Cl)_2$ in acetonitrile solution, due to a similar equilibrium as shown for the TPPh complex in Scheme 1. The P-donor in the TPAMP ligand appears to have a much stronger *trans* effect compared to TPPh, resulting in a highly labile chloro ligand, and consequently the equilibrium is shifted toward the dicationic complex.

Subsequent reactions with $AgSbF_6$ in acetonitrile result in the dicationic complexes $[Ru(MeCN)_3(TPPh)](SbF_6)_2$ and $[Ru(MeCN)_3(TPAMP)](SbF_6)_2$. Also in these complexes the TPPh and TPAMP ligands remain coordinated as tridentate rather than tetradentate ligands. The ^1H NMR spectrum of $[Ru(MeCN)_3(TPPh)](SbF_6)_2$ at 298 K in CD_3CN shows two different environments for the pyridine and the CH_2 protons, both in a ratio of 2:1. The CH_2 protons from the uncoordinated pyridine appear as a doublet at δ 4.06 ppm with $^2J_{HP}$ = 12.6 Hz. The diastereotopic CH_2 protons of the coordinated pyridines appear as two double doublets at δ 4.14 and δ 3.88 ppm, with $^2J_{HH}$ = 18.4 Hz, $^2J_{HP}$ = 11, and $^2J_{HP}$ =15 Hz, respectively. The acetonitrile ligands give two singlet resonances: one integrates to six protons and the other to three protons, and the latter is coordinated *trans* to phosphorus. This acetonitrile ligand exchanges with the solvent CD_3CN during the course of several hours at room temperature. VT ^1H and ^{31}P NMR measurements have shown no evidence for other dynamic behavior of this complex over the temperature range from 243 to 343 K.

In the ^1H NMR spectrum of $[Ru(MeCN)_3(TPAMP)](SbF_6)_2$, the coordinated pyridines give four resonances, and the uncoordinated pyridine gives a separate set of four resonances. There are two doublets for the aminomethyl groups at δ 3.50 and 3.15 ppm, with $^3J_{HP}$ = 5.9 Hz for the coordinated pyridines and $^3J_{HP}$ = 9.5 Hz for the uncoordinated pyridine. The exchange of the CH_3CN ligand *trans* to P for CD_3CN occurs within 10 min, significantly faster than for $[Ru(MeCN)_3(TPPh)](SbF_6)_2$, which required several hours for complete exchange. This is most likely due to the stronger *trans* effect of the phosphorus donor in TPAMP compared to TPPh. The $^{31}P\{^1H\}$ NMR spectrum displays a single resonance at δ 165.1 ppm (Figure S13).

dx.doi.org/10.1021/ic4005196 | *Inorg. Chem.* 2013, 52, 7000−7009

Scheme 1

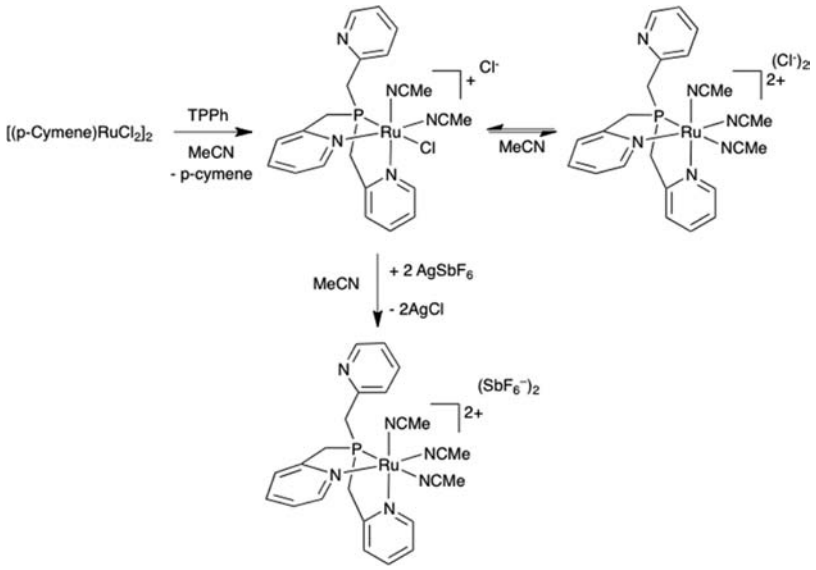

Single crystals of $[Ru(MeCN)_3(TPPh)](SbF_6)_2$, suitable for single crystal X-ray crystallography, were obtained by layering an acetonitrile solution of the complex with diethyl ether. The structure obtained and selected bond lengths and angles are shown in Figure 8. Complex $[Ru(MeCN)_3(TPPh)](SbF_6)_2$ crystallized with two independent cations (and four independent anions) in the asymmetric unit; the two cations are very similar, with the rms fit of all the non-hydrogen atoms of the two complexes being *ca.* 0.05 Å. The TPPh ligand binds in a tridentate fashion; the M−P−CH_2 angle involving the noncoordinated arm is substantially larger [128.1(3)° and 128.3(3)°] than those for the coordinated arms [in the range 101.7(4)−105.1(3)°].

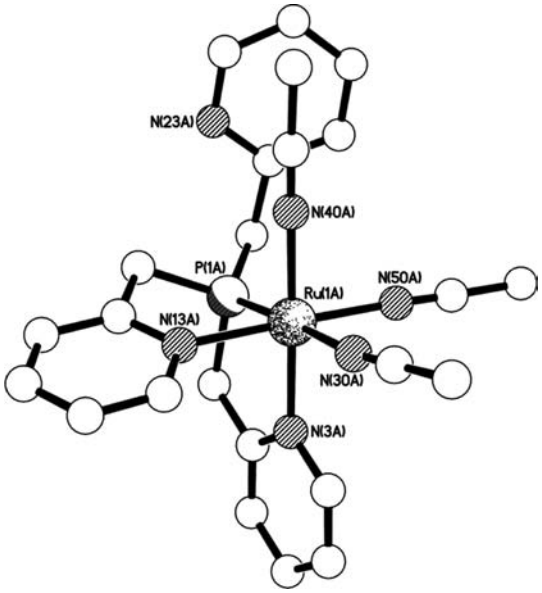

Figure 8. Structure of one (A) of the two independent cations present in the crystals of $[Ru(MeCN)_3(TPPh)](SbF_6)_2$. Selected bond lengths (Å) and angles (deg) (values in square brackets refer to cation B): Ru(1A)−P(1A) 2.210(2) [2.208(2)], Ru(1A)−N(3A) 2.098(6) [2.095(6)], Ru(1A)−N(13A) 2.085(7) [2.095(7)], P(1A)−Ru(1A)−N(3A) 83.53(17) [83.98(18)], P(1A)−Ru(1A)−N(13A) 80.8(2) [81.18(19)], N(3A)−Ru(1A)−N(13A) 86.8(3) [88.1(2)].

The TPPh and TPAMP ligands in the complexes presented here coordinate in all cases in a tridentate fashion with one of the pyridyl arms not coordinated, which is in stark contrast to related TPA complexes, where the TPA ligand typically coordinates in a tetradentate mode. The hypodentate coordination behavior[63] of TPPh and TPAMP is believed to be a consequence of the larger M−P distances, which are typically 7−8% larger than the M−N distances in related TPA complexes (see Table S1). In TPA complexes, all three pyridylmethyl arms can normally reach the metal and result in a tetradentate coordination mode, although this typically results in two smaller and one large M−N−CH_2 angle. In some cases, the third arm cannot effectively bind to the metal center, and the TPA ligand coordinates as a tridentate ligand.[4−8]

Cyclic Voltammetry and UV−Vis Spectroscopy. Cyclic voltammetry measurements have been carried out in MeCN under N_2 at room temperature with 0.1 M $[NBu_4][PF_6]$ as the electrolyte. The dicationic complex $[Ru(MeCN)_2(TPA)](SbF_6)_2$ displays pseudoreversible redox behavior with $E_{1/2}$ = 1.31 V (vs Ag/AgCl) for the Ru(II)/Ru(III) redox couple (Figure 9). This value is higher compared to related monocationic ruthenium(II) TPA complexes such as $[RuCl(DMSO)(TPA)]PF_6$ ($E_{1/2}$ = 0.98 V, vs Ag/AgCl) or $[RuCl(PhCN)(TPA)]Cl$ ($E_{1/2}$ = 0.77 V, vs Ag/AgCl), both of which contain anionic chloro ligands which lower the redox potential.[25] Further oxidation to Ru(IV) is not observed for $[Ru(MeCN)_2(TPA)](SbF_6)_2$, similar to observations with the other ruthenium(II) TPA complexes. It is noteworthy that the Ru(III)/Ru(IV) redox couple has been observed for ruthenium(III) TPA complexes such as $[RuCl_2(TPA)]^+$ at $E_{1/2}$ = 1.73 V (vs Ag/AgCl), which contains two chloro ligands.[20,62]

The Ru(II)/Ru(III) redox potential is observed at $E_{1/2}$ = 1.47 V for $[Ru(MeCN)_3(TPAMP)](SbF_6)_2$ and at a slightly lower potential for $[Ru(MeCN)_3(TPPh)](SbF_6)_2$ (Figure 9). Changing the nitrogen amine donor in TPA for a strong field P-donor (and one pyridine ligand for an acetonitrile ligand) increases the Ru(II)/Ru(III) redox potential considerably. Interestingly, a further Ru(III)−Ru(IV) redox couple is

dx.doi.org/10.1021/ic4005196 | *Inorg. Chem.* 2013, 52, 7000−7009

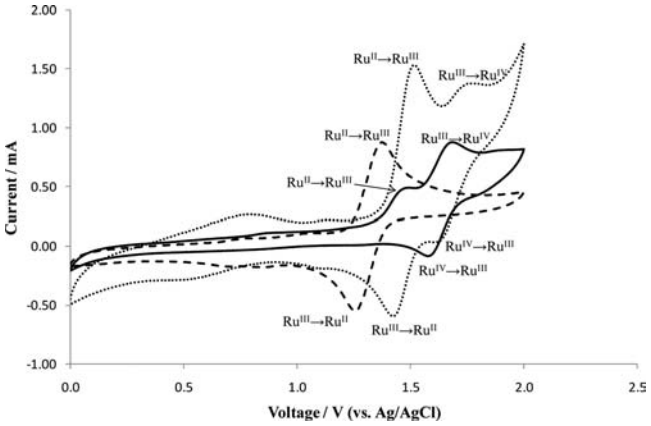

Figure 9. Cyclic voltammograms of $[Ru(MeCN)_2(TPA)](SbF_6)_2$ (- - -), $[Ru(MeCN)_3(TPPh)](SbF_6)_2$ (—), and $[Ru(MeCN)_3(TPAMP)](SbF_6)_2$ (···): 1 mM in acetonitrile, 0.1 M $[NBu_4][PF_6]$ vs Ag/AgCl.

observed, which is pseudoreversible for both the TPPh and the TPAMP complex with $E_{1/2}$ values of 1.63 and 1.69 V, respectively. These results suggest that high valent ruthenium(IV) oxo TPPh and TPAMP complexes might become accessible upon oxidation of the ruthenium(II) complexes with a suitable oxidant. This has been investigated in the next section.

The substitution of acetonitrile ligands for anionic weak field chloro ligands generally lowers the redox potential. This is seen here for $[RuCl(MeCN)_2(TPPh)]Cl$, where the Ru(II)/Ru(III) redox process occurs at ca. 1.0 V, compared to ca. 1.4 V in the case of $[Ru(MeCN)_3(TPPh)](SbF_6)_2$ (both irreversible, see Figure 10). The Ru(III)/Ru(IV) redox process occurs at $E_{1/2}$ =

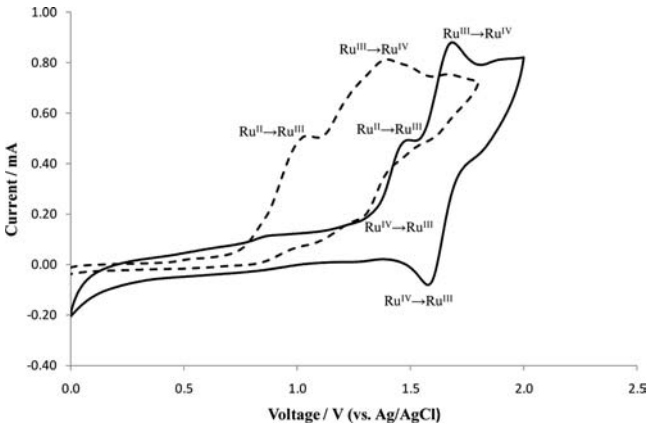

Figure 10. Cyclic voltammograms of $[RuCl(MeCN)_2(TPP)]Cl$ (- - -) and $[Ru(MeCN)_3(TPPh)](SbF_6)_2$ (—): 1 mM in CH_3CN, 0.1 M $[NBu_4][PF_6]$, vs Ag/AgCl.

1.32 V, compared to $E_{1/2}$ = 1.63 V for $[Ru(MeCN)_3(TPPh)](SbF_6)_2$. A similar trend is seen when comparing $[RuCl(MeCN)_2(TPAMP)]Cl$ and $[Ru(MeCN)_3(TPAMP)](SbF_6)_2$, where the results for the Ru(II)/Ru(III) redox potentials are $E_{1/2}$ = 0.95 and 1.47 V, respectively, and the Ru(III)/Ru(IV) potentials are observed at ca. $E_{1/2}$ = 1.3 V (irreversible) and 1.69 V, respectively (see Figure S14).

The UV–vis spectra of $[Ru(MeCN)_2(TPA)](SbF_6)_2$, $[Ru(MeCN)_3(TPPh)](SbF_6)_2$, and $[Ru(MeCN)_3(TPAMP)](SbF_6)_2$ in acetonitrile at 298 K are shown in Figure 11. The

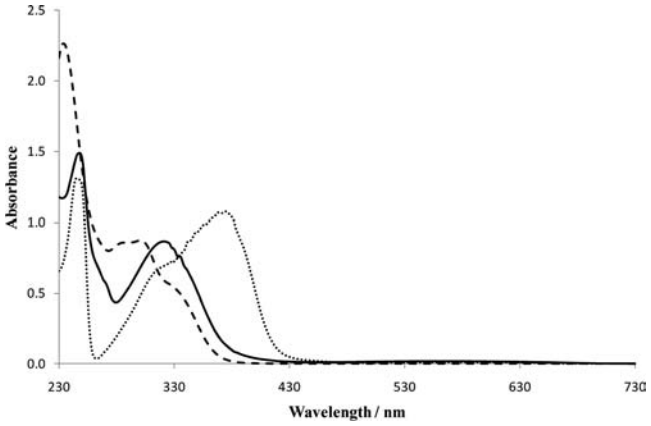

Figure 11. UV–vis spectra of $[Ru(MeCN)_2(TPA)](SbF_6)_2$ (···), $[Ru(MeCN)_3(TPPh)](SbF_6)_2$ (—), and $[Ru(MeCN)_3(TPAMP)](SbF_6)_2$ (- - -); c = 0.5 mM in CH_3CN at 298 K.

spectrum of $[Ru(MeCN)_2(TPA)](SbF_6)_2$ shows two MLCT bands at λ_{max} = 371 nm (ε = 2200 M^{-1} cm^{-1}) and a distinct shoulder at 316 nm (ε = 1400 M^{-1} cm^{-1}), probably due to the two different pyridine environments. The complexes $[Ru(MeCN)_3(TPPh)](SbF_6)_2$ and $[Ru(MeCN)_3(TPAMP)](SbF_6)_2$, where only two of the three pyridine donors are coordinated, show only one MLCT band at λ_{max} = 318 nm (ε = 1900 M^{-1} cm^{-1}) and 299 nm (ε = 1900 M^{-1} cm^{-1}), respectively.

Ruthenium Oxo Complexes and Oxidation Studies. High valent ruthenium oxo complexes are often invoked as intermediates in ruthenium-based oxidation catalysis.[64] Several stable ruthenium(IV) oxo complexes have been isolated and characterized, for example $[Ru(O)(bipy)_2(py)]^{2+}$ (bipy = 2,2′-bipyridine),[65–72] $[Ru(O)(terpy)(bipy)]^{2+}$ (terpy = 2,2′,6′,2″-terpyridine),[73–75] and $[Ru(O)(terpy)(pic)]^{+}$ (pic = picolinate).[76] Ruthenium(IV)-oxo TPA complexes have been prepared by the oxidation of ruthenium(II) complexes using a suitable oxidizing agent such as cerium(IV) ammonium nitrate (CAN), as was previously shown for the oxidation of $[Ru(H_2O)_2(TPA)](PF_6)_2$ to give the mononuclear ruthenium(IV) complex $[Ru(O)(H_2O)(TPA)](PF_6)_2$.[23] Catalytic oxidation reactions of various hydrocarbons have been described using ruthenium TPA complexes in combination with oxidants such as *meta*-chloroperoxybenzoic acid (*m*-CPBA).[20,25,26]

Attempts to generate high valent ruthenium oxo complexes were made by reacting $[Ru(MeCN)_2(TPA)](SbF_6)_2$ in acetonitrile with an excess of *m*-CPBA (10 equiv). The UV–vis spectrum shows a gradual change during the course of 30 min, as shown in Figure 12. The analogous reaction of $[Ru(MeCN)_3(TPPh)](SbF_6)_2$ with 10 equiv of *m*-CPBA in acetonitrile results in a slow color change to give a rather featureless UV–vis spectrum with no clearly discernible absorptions (Figure S16). Similarly, the addition of *m*-CPBA to a solution of $[Ru(MeCN)_3(TPAMP)](SbF_6)_2$ in acetonitrile showed a very slow change over several hours to give again a featureless spectrum (Figure S17).

The formation of a shoulder in the UV–vis spectrum around 500 nm upon oxidation of $[Ru(MeCN)_2(TPA)](SbF_6)_2$ with *m*-CPBA is similar to the observations reported for the reaction of $[Ru(H_2O)_2(TPA)](PF_6)_2$ with CAN, which resulted in the formation of the ruthenium(IV) oxo complex $[Ru(O)(H_2O)(TPA)](PF_6)_2$ (see Figure S15).[23] Analysis of the reaction mixture by mass spectrometry (LSIMS) also showed the

dx.doi.org/10.1021/ic4005196 | *Inorg. Chem.* 2013, 52, 7000–7009

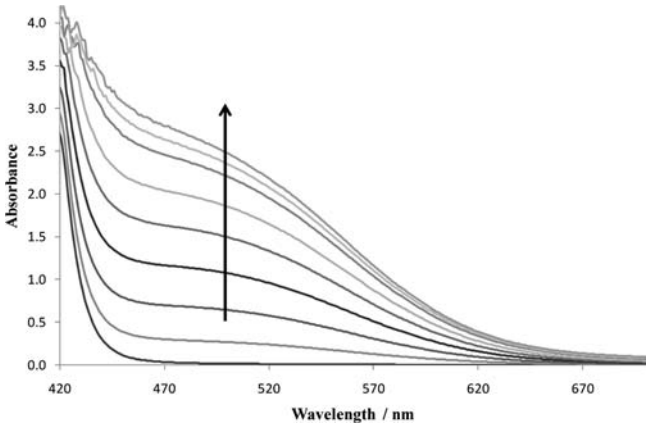

Figure 12. UV−vis spectrum of $[Ru(TPA)(MeCN)_2](SbF_6)_2$ (5 mM) after addition of 10 equiv of *m*-CPBA in acetonitrile at 298 K. Readings taken every 3 min.

formation of a ruthenium oxo species (see Figure S18), and we therefore conclude that a ruthenium(IV) oxo complex $[Ru(O)(MeCN)(TPA)](SbF_6)_2$ is probably generated as a transient complex when TPA is the supporting ligand. In the case of TPPh and TPAMP, the results are less clear. It is possible that upon reaction with *m*-CPBA a ruthenium(IV) oxo complex is formed, but immediate reaction with the ruthenium(II) starting complex could result in oxo-bridged dinuclear ruthenium(III) complexes such as $[\{Ru(MeCN)_2(TPPh)\}_2(\mu\text{-}O)]^{4+}$ or $[\{Ru(MeCN)(TPPh)\}_2(\mu\text{-}O)(\mu\text{-}meta\text{-}chlorobenzoate)]^{3+}$. Complexes of this type, for example $[\{RuCl(TPA)\}_2(\mu\text{-}O)]^{2+}$ and $[\{Ru(TPA)\}_2(\mu\text{-}O)(\mu\text{-}acetate)]^{3+}$, have been previously isolated and crystallographically characterized by Sasaki and co-workers.[77]

Although cyclic voltammetry studies have shown that the ruthenium(II) complexes containing TPPh and TPAMP can be electrochemically oxidized to ruthenium(IV), the strong field TPPh and TPAMP ligands are probably unable to sufficiently

Table 1. Crystallographic Data for Compounds $[CrCl_3(TPPh)]$, $[Fe(TPPh)_2][FeBr_4]$, $[Fe(TPAMP)_2](OTf)_2$, $[Fe(TPAMP)_2][FeCl_4]_2$, $[RuCl_2(TPA)]$, $[Ru(MeCN)_2(TPA)](SbF_6)_2$, and $[Ru(MeCN)_3(TPPh)](SbF_6)_2$

	$[CrCl_3(TPPh)]$	$[Fe(TPPh)_2][FeBr_4]$	$[Fe(TPAMP)_2](OTf)_2$	$[Fe(TPAMP)_2][FeCl_4]_2$
chemical formula	$C_{18}H_{18}Cl_3CrN_3P$	$[C_{36}H_{36}FeN_6P_2](FeBr_4)$	$[C_{36}H_{42}FeN_{12}P_2](CF_3SO_3)_2$	$[C_{36}H_{42}FeN_{12}P_2](FeCl_4)_2$
solvent		CH_3CN	CH_2Cl_2	
fw	465.67	1087.04	1143.67	1155.91
T (°C)	−100	−100	−100	−100
space group	$P2_1/c$ (No. 14)	*Ibca* (No. 73)	$P\bar{1}$ (No. 2)	$P2_1/n$ (No. 14)
a (Å)	12.072 64(15)	19.8229(2)	13.1348(3)	21.5022(2)
b (Å)	9.898 70(11)	22.6568(3)	13.5183(3)	32.0677(2)
c (Å)	17.5667(2)	18.5048(2)	14.2438(3)	29.0228(2)
α (deg)			92.8540(17)	
β (deg)	104.6450(13)		97.9214(18)	104.3814(9)
γ (deg)			104.5567(18)	
V (Å^3)	2031.08(4)	8310.94(16)	2415.17(10)	19 384.9(3)
Z	4	8	2	16[a]
ρ_{calcd} (g cm^{-3})	1.523	1.738	1.573	1.584
λ (Å)	0.710 73	1.541 84	0.710 73	0.710 73
μ (mm^{-1})	1.044	11.129	0.658	1.435
R1 (obsd)[c]	0.0283	0.0384	0.0596	0.0626
wR2 (all)[d]	0.0765	0.1017	0.1763	0.1811

	$[RuCl_2(TPA)]$	$[Ru(MeCN)_2(TPA)](SbF_6)_2$	$[Ru(MeCN)_3(TPPh)](SbF_6)_2$
chemical formula	$C_{18}H_{18}Cl_2N_4Ru$	$[C_{22}H_{24}N_6Ru](SbF_6)_2$	$[C_{24}H_{27}N_6PRu](SbF_6)_2$
solvent	$3CH_2Cl_2$	CH_3CN	$0.5C_4H_{10}O{\cdot}0.5CH_3CN$
fw	717.11	986.10	1060.64
T (°C)	−100	−100	−100
space group	$P2_1/c$ (No. 14)	$P\bar{1}$ (No. 2)	$P2_1/n$ (No. 14)
a (Å)	8.543 32(10)	8.710 65(14)	10.7301(3)
b (Å)	24.0817(3)	9.043 39(16)	37.0357(11)
c (Å)	13.862 64(17)	20.2295(3)	20.8357(10)
α (deg)		93.6493(14)	
β (deg)	96.5352(11)	93.6436(14)	101.078(4)
γ (deg)		92.6472(14)	
V (Å^3)	2833.54(6)	1585.09(4)	8125.8(5)
Z	4	2	8[b]
ρ_{calcd} (g cm^{-3})	1.681	2.066	1.734
λ (Å)	0.710 73	0.710 73	1.541 84
μ (mm^{-1})	1.327	2.262	14.579
R1 (obsd)[c]	0.0359	0.0284	0.0737
wR2 (all)[d]	0.0767	0.0575	0.2349

[a]There are four crystallographically independent complexes in the asymmetric unit. [b]There are two crystallographically independent complexes in the asymmetric unit. [c]$R1 = \Sigma||F_o| - |F_c||/\Sigma|F_o|$. [d]$wR2 = \{\Sigma[w(F_o^2 - F_c^2)^2]/\Sigma[w(F_o^2)^2]\}^{1/2}$; $w^{-1} = \sigma^2(F_o^2) + (aP)^2 + bP$.

dx.doi.org/10.1021/ic4005196 | *Inorg. Chem.* 2013, 52, 7000−7009

stabilize the high valent oxo complexes. Rapid reduction by the ruthenium(II) starting complex to give an oxo-bridged dinuclear ruthenium(III) complex is a conceivable decomposition pathway. In fact, there are parallels for this behavior in iron(II) complexes. We and others have reported very similar observations with low spin iron(II) complexes containing strong field ligands. Iron(IV) oxo complexes, generated from iron(II) complexes upon oxidation with PhIO, were rapidly reduced by the iron(II) starting complex to oxo-bridged dinuclear iron(III) complexes.[78,79] Strong field ligands with π-acceptor properties are inherently unsuited for the stabilization of high valent metal oxo complexes and ligands with strong σ- and π-donor properties should be used.

Oxidation reactions of various hydrocarbons have been described using ruthenium-TPA catalysts in combination with oxidants such as *m*-CPBA.[20,25,26] We have carried out oxidation reactions of both cyclohexene and cyclohexane using iodosylbenzene or hydrogen peroxide as the oxidants and $[Ru(MeCN)_2(TPA)](SbF_6)_2$ or $[Ru(MeCN)_3(TPPh)](SbF_6)_2$ as the catalyst. Under our reaction conditions, no oxidation of cyclohexane with hydrogen peroxide was observed when using any of the ruthenium(II) complexes. The oxidation of cyclohexene by iodosylbenzene gave trace amounts of cyclohexene oxide and a bis-chlorinated cyclohexane product, when the reaction was carried out in chloroform as the solvent. Formation of chlorinated species indicates that a radical intermediate is generated under these reaction conditions. Once the solvent was changed to a nonchlorinated solvent, such as acetonitrile, only very low yields of cyclohexene oxide were observed.

CONCLUSIONS

The first successful synthesis of tri(pyridylmethyl)phosphine, TPPh, has been achieved, the congener of the well-known TPA ligand. Chromium(III), iron(II), and ruthenium(II) complexes have been prepared, and the coordination behavior of TPPh has been compared with TPA. In all complexes prepared in this study, the TPPh ligand acts as a tridentate ligand, whereas TPA most commonly acts as a tetradentate ligand, although several tridentate examples are known. The main reason for the hypodentate coordination behavior[63] is the longer M−P bond distance compared to M−N, allowing only two pyridyl units to comfortably coordinate to the metal center. The third pyridine unit could be used for further coordination to give multimetallic complexes, or for metal−ligand cooperativity in catalytic reactions.

In the case of iron(II), low spin bis(ligand) complexes were obtained with TPPh and TPAMP, whereas ruthenium(II) gave complexes with only one ligand. Cyclic voltammetry studies have indicated that Ru(III) and Ru(IV) complexes should be accessible upon oxidation. However, no high valent ruthenium(IV) oxo complexes could be isolated upon oxidation with *m*-CPBA. The strong field TPPh and TPAMP ligands are believed to destabilize high oxidation states, resulting in rapid decomposition, probably to the well-known oxo-bridged ruthenium(III) complexes.

EXPERIMENTAL SECTION

Crystallographic Details. Table 1 provides a summary of the crystallographic data for compounds $[CrCl_3(TPPh)]$, $[Fe(TPPh)_2][FeBr_4]$, $[Fe(TPAMP)_2](OTf)_2$, $[Fe(TPAMP)_2][FeCl_4]_2$, $[RuCl_2(TPA)]$, $[Ru(MeCN)_2(TPA)](SbF_6)_2$, and $[Ru(MeCN)_3(TPPh)](SbF_6)_2$. Data were collected using Oxford Diffraction Xcalibur PX Ultra (compounds $[Fe(TPPh)_2][FeBr_4]$ and $[Ru(MeCN)_3(TPPh)](SbF_6)_2$) and Xcalibur 3 (compounds $[CrCl_3(TPPh)]$, $[Fe(TPAMP)_2](OTf)_2$, $[Fe(TPAMP)_2][FeCl_4]_2$, $[RuCl_2(TPA)]$ and $[Ru(MeCN)_2(TPA)](SbF_6)_2$) diffractometers, and the structures were refined on the basis of F^2 using the SHELXTL and SHELX-97 program systems.[80] CCDC 926471 to 926477 contain the relevant data.

ASSOCIATED CONTENT

Supporting Information

X-ray crystallographic files in CIF format for all complexes and experimental details regarding synthesis and characterization of the ligands and complexes, as well as details on the electrochemical, spectroscopic, and catalytic procedures. This material is available free of charge via the Internet at http://pubs.acs.org.

AUTHOR INFORMATION

Corresponding Author

*E-mail: g.britovsek@imperial.ac.uk. Phone: +44-(0)20-75945863. Fax. +44-(0)-20-75945804.

Notes

The authors declare no competing financial interest.

ACKNOWLEDGMENTS

We are grateful to EPSRC for financial support. E.K. thanks the British Council for his placement under the IEASTE scheme. We thank Johnson Matthey for the generous loan of ruthenium trichloride, and we thank Prof. G. Cloke, University of Sussex, for the kind donation of tris(trimethylsilyl)phosphine.

REFERENCES

(1) Blackman, A. G. *Eur. J. Inorg. Chem.* **2008**, 2633−2647.
(2) Blackman, A. G. *Polyhedron* **2005**, *24*, 1−39.
(3) Anderegg, G.; Wenk, F. *Helv. Chim. Acta* **1967**, *50*, 2330−2332.
(4) Sugimoto, H.; Sasaki, Y. *Chem. Lett.* **1997**, 541−542.
(5) Diebold, A.; Hagen, K. S. *Inorg. Chem.* **1998**, *37*, 215−223.
(6) Bjernemose, J.; Hazell, A.; McKenzie, C. J.; Mahon, M. F.; Nielsen, L. P.; Raithby, P. R.; Simonsen, O.; Toftlund, H.; Wolny, J. A. *Polyhedron* **2003**, *22*, 875−885.
(7) Kojima, T.; Sakamoto, T.; Matsuda, Y. *Inorg. Chem.* **2004**, *43*, 2243−2245.
(8) Kojima, T.; Morimoto, T.; Sakamoto, T.; Miyazaki, S.; Fukuzumi, S. *Chem.−Eur. J.* **2008**, *14*, 8904−8915.
(9) Højland, F.; Toftlund, H.; Yde-Andersen, S. *Acta Chem. Scand.* **1983**, *A 37*, 251−257.
(10) Davies, C. J.; Solan, G. A.; Fawcett, J. *Polyhedron* **2004**, *23*, 3105−3114.
(11) Chen, K.; Costas, M.; Kim, J.; Tipton, A.; Que, L., Jr. *J. Am. Chem. Soc.* **2002**, *124*, 3026−3035.
(12) Chen, K.; Que, L., Jr. *J. Am. Chem. Soc.* **2001**, *123*, 6327−6337.
(13) Kim, C.; Chen, K.; Kim, J.; Que, L., Jr. *J. Am. Chem. Soc.* **1997**, *119*, 5964−5965.
(14) Mairata i Payeras, A.; Ho, R. Y. N.; Fujita, M.; Que, L., Jr. *Chem.−Eur. J.* **2004**, *10*, 4944−4953.
(15) Zang, Y.; Kim, J.; Dong, Y.; Wilkinson, E. C.; Appelman, E. H.; Que, L., Jr. *J. Am. Chem. Soc.* **1997**, *119*, 4197−4205.
(16) Fujita, M.; Costas, M.; Que, L., Jr. *J. Am. Chem. Soc.* **2003**, *125*, 9912−9913.
(17) Bassan, A.; Blomberg, M. R. A.; Siegbahn, P. E. M.; Que, L., Jr. *Chem.−Eur. J.* **2005**, *11*, 692−705.
(18) Mandon, D.; Machkour, A.; Goetz, S.; Welter, R. *Inorg. Chem.* **2002**, *41*, 5364−5372.
(19) Britovsek, G. J. P.; England, J.; White, A. J. P. *Inorg. Chem.* **2005**, *44*, 8125−8134.
(20) Kojima, T. *Chem. Lett.* **1996**, 121−122.

(21) Kojima, T.; Matsuda, Y. *Chem. Lett.* **1999**, 81−82.
(22) Kojima, T.; Matsuo, H.; Matsuda, Y. *Inorg. Chim. Acta* **2000**, *300*−*302*, 661−667.
(23) Hirai, Y.; Kojima, T.; Mizutani, Y.; Shiota, Y.; Yoshizawa, K.; Fukuzumi, S. *Angew. Chem., Int. Ed.* **2008**, *47*, 5772−5776.
(24) Kojima, T.; Hirai, Y.; Ishizuka, T.; Shiota, Y.; Yoshizawa, K.; Ikemura, K.; Ogura, T.; Fukuzumi, S. *Angew. Chem., Int. Ed.* **2010**, *49*, 8449−8453.
(25) Yamaguchi, M.; Kousaka, H.; Izawa, S.; Ichii, Y.; Kumano, T.; Masui, D.; Yamagishi, T. *Inorg. Chem.* **2006**, *45*, 8342−8354.
(26) Yamaguchi, M.; Kousaka, H.; Yamagishi, T. *Chem. Lett.* **1997**, 769−770.
(27) Nagataki, T.; Tachi, Y.; Itoh, S. *Chem. Commun.* **2006**, 4016−4018.
(28) Lim, M. H.; Rohde, J.-U.; Stubna, A.; Bukowski, M. R.; Costas, M.; Ho, R. Y. N.; Münck, E.; Nam, W.; Que, L., Jr. *Proc. Natl. Acad. Sci. U.S.A.* **2003**, *100*, 3665−3670.
(29) Che, C.-M.; Yam, V. W.-W. *J. Am. Chem. Soc.* **1990**, *112*, 2284−2291.
(30) Che, C.-M.; Ho, C.; Lau, T.-C. *J. Chem. Soc., Dalton Trans.* **1991**, 1901−1905.
(31) Jitsukawa, K.; Oka, Y.; Yamaguchi, S.; Masuda, H. *Inorg. Chem.* **2004**, *43*, 8119−8129.
(32) Radaram, B.; Ivie, J. A.; Marjit Singh, W.; Grudzien, R. M.; Reibenspies, J. H.; Webster, C. E.; Zhao, X. *Inorg. Chem.* **2011**, *50*, 10564−10571.
(33) Kojima, T.; Nakayama, K.; Ikemura, K.; Ogura, T.; Fukuzumi, S. *J. Am. Chem. Soc.* **2011**, *133*, 11692−11700.
(34) Romero, I.; Rodriguez, M.; Sens, C.; Mola, J.; Kollipara, M. R.; Francas, L.; Mas-Marza, E.; Escriche, L.; Llobet, A. *Inorg. Chem.* **2008**, *47*, 1824−1834.
(35) Kalita, D.; Radaram, B.; Brooks, B.; Kannam, P. P.; Zhao, X. *ChemCatChem* **2011**, *3*, 561−570.
(36) Li, F.; Yu, M.; Jiang, Y.; Huang, F.; Li, Y.; Zhang, B.; Sun, L. *Chem. Commun.* **2011**, *47*, 8949−8951.
(37) Merkel, M.; Pascaly, M.; Krebs, B.; Astner, J.; Foxon, S. P.; Schindler, S. *Inorg. Chem.* **2005**, *44*, 7582−7589.
(38) The abbreviation tpp for tri(pyridylmethyl)phosphine was used in ref 39. To avoid confusion with tetraphenylporphyrin, we have changed the abbreviation to TPPh.
(39) Chiswell, B. *Aust. J. Chem.* **1967**, *20*, 2533−2534.
(40) Knebel, W. J.; Angelici, R. J. *Inorg. Chim. Acta* **1973**, *7*, 713−716.
(41) tom Dieck, H.; Hahn, G. *Z. Anorg. Allg. Chem.* **1989**, *577*, 74−82.
(42) Uhlig, E.; Schäfer, M. *Z. Anorg. Allg. Chem.* **1968**, *359*, 67−77.
(43) Schäfer, M.; Uhlig, E. *Z. Anorg. Allg. Chem.* **1974**, *407*, 23−34.
(44) Lindner, E.; Rauleder, H.; Hiller, W. *Z. Naturforsch.* **1983**, *38B*, 417−425.
(45) Klausmeyer, K. K.; Hung-Low, F. *Acta Crystallogr., Sect. E* **2006**, *62*, m2415−2416.
(46) Liu, S.; Peloso, R.; Pattacini, R.; Braunstein, P. *Dalton Trans.* **2010**, *39*, 7881−7883.
(47) Hung-Low, F.; Renz, A.; Klausmeyer, K. K. *Eur. J. Inorg. Chem.* **2009**, 2994−3002.
(48) Liu, S.; Peloso, R.; Braunstein, P. *Dalton Trans.* **2010**, *39*, 2563−2572.
(49) Liu, S.; Pattacini, R.; Braunstein, P. *Organometallics* **2011**, *30*, 3549−3558.
(50) Casares, J. A.; Espinet, P.; Soulantica, K.; Pascual, I.; Orpen, A. G. *Inorg. Chem.* **1997**, *36*, 5251−5256.
(51) Tolman, C. A.; Druliner, J. D.; Krusic, P. J.; Nappa, M. J.; Seidel, W. C.; Williams, I. D.; Ittel, S. D. *J. Mol. Catal.* **1988**, *48*, 129−148.
(52) Seidel, W.; Schöler, H. *Z. Chem.* **1967**, *7*, 431.
(53) Ainscough, E. W.; Peterson, L. K. *Inorg. Chem.* **1970**, *9*, 2699−2705.
(54) Aucott, S. M.; Slawin, A. M. Z.; Woollins, J. D. *J. Chem. Soc., Dalton Trans.* **2000**, 2559−2575.
(55) Fischbach, U.; Rüegger, H.; Grützmacher, H. *Eur. J. Inorg. Chem.* **2007**, 2654−2667.
(56) Herberhold, M.; Bauer, K.; Milius, W. *Z. Anorg. Allg. Chem.* **1994**, *620*, 2108−2113.
(57) Lindner, E.; Scheytt, C. *Z. Naturforsch.* **1985**, *41B*, 10−17.
(58) Kermagoret, A.; Tomicki, F.; Braunstein, P. *Dalton Trans.* **2008**, 2945−2955.
(59) Robertson, N. J.; Carney, M. J.; Halfen, J. A. *Inorg. Chem.* **2003**, *42*, 6876−6885.
(60) Nobbs, J. D.; Tomov, A. K.; Cariou, R.; Gibson, V. C.; White, A. J. P.; Britovsek, G. J. P. *Dalton Trans.* **2012**, *41*, 5949−5964.
(61) Smit, T. M.; Tomov, A. K.; Britovsek, G. J. P.; Gibson, V. C.; White, A. J. P.; Williams, D. J. *Catal. Sci. Technol.* **2012**, *2*, 643−655.
(62) Kojima, T.; Amano, T.; Ishii, Y.; Ohba, M.; Okaue, Y.; Matsuda, Y. *Inorg. Chem.* **1998**, *37*, 4076−4085.
(63) Constable, E. C. *Prog. Inorg. Chem.* **1994**, *42*, 67−138.
(64) Griffith, W. P. *Ruthenium Oxidation Complexes*; Springer: New York, 2010.
(65) Moyer, B. A.; Meyer, T. J. *Inorg. Chem.* **1981**, *20*, 436−444.
(66) Moyer, B. A.; Sipe, B. K.; Meyer, T. J. *Inorg. Chem.* **1981**, *20*, 1475−1480.
(67) Roecker, L.; Dobson, J. C.; Vining, W. J.; Meyer, T. J. *Inorg. Chem.* **1987**, *26*, 779−781.
(68) Roecker, L.; Meyer, T. J. *J. Am. Chem. Soc.* **1987**, *109*, 746−754.
(69) Stultz, L. K.; Binstead, R. A.; Reynolds, M. S.; Meyer, T. J. *J. Am. Chem. Soc.* **1995**, *117*, 2520−2532.
(70) Stultz, L. K.; Huynh, M. H. V.; Binstead, R. A.; Curry, M.; Meyer, T. J. *J. Am. Chem. Soc.* **2000**, *122*, 5984−5996.
(71) Bryant, J. R.; Mayer, J. M. *J. Am. Chem. Soc.* **2003**, *125*, 10351−10361.
(72) Seok, W. K.; Meyer, T. J. *J. Am. Chem. Soc.* **1988**, *110*, 7358−7367.
(73) Moyer, B. A.; Thompson, M. S.; Meyer, T. J. *J. Am. Chem. Soc.* **1980**, *102*, 2310−2312.
(74) Thompson, M. S.; Meyer, T. J. *J. Am. Chem. Soc.* **1982**, *104*, 4106−4115.
(75) Seok, W. K.; Meyer, T. J. *Inorg. Chem.* **2005**, *44*, 3931−3941.
(76) Chatterjee, D. *Inorg. Chim. Acta* **2008**, *361*, 2177−2182.
(77) Koshi, C.; Umakoshi, K.; Sasaki, Y. *Chem. Lett.* **1997**, 1155−1156.
(78) Wong, E.; Jeck, J.; Grau, M.; White, A. J. P.; Britovsek, G. J. P. *Catal. Sci. Technol.* **2013**, *3*, 1116−1122.
(79) Balland, V.; Charlot, M.-F.; Banse, F.; Girerd, J.-J.; Mattioli, T. A.; Bill, E.; Bartoli, J. F.; Battioni, P.; Mansuy, D. *Eur. J. Inorg. Chem.* **2004**, 301−308.
(80) Sheldrick, G. M. *Acta Crystallogr.* **2008**, *A64*, 112−122.